Journal of Magnetic Resonance **143,** 435–439 (2000)
doi:10.1006/jmre.2000.2058, available online at http://www.idealibrary.com on IDEAL®

# Magnetization Transfer via Residual Dipolar Couplings: Application to Proton–Proton Correlations in Partially Aligned Proteins

Maurizio Pellecchia,*[,1,2] Craig W. Vander Kooi,† Kai Keliikuli,* and Erik R. P. Zuiderweg*[,†,‡,2]

*Biophysics Research Division, †Department of Chemistry, and ‡Department of Biological Chemistry, The University of Michigan, 930 North University Avenue, Ann Arbor, Michigan 48109

Received February 10, 2000

**A novel three-dimensional NMR experiment is reported that allows the observation of correlations between amide and other protons via residual dipolar couplings in partially oriented proteins. The experiment is designed to permit quantitative measurement of the magnitude of proton–proton residual dipolar couplings in larger molecules and at higher degree of alignments. The observed couplings contain data valuable for protein resonance assignment, local protein structure refinement, and determination of low-resolution protein folds.** © 2000 Academic Press

*Key Words:* **residual dipolar coupling; protein structure; protein assignment; homonuclear decoupling.**

Residual one- and two-bond heteronuclear dipolar couplings provide novel constraints for protein structure refinement in high-resolution solution NMR (*1–7*). These couplings are commonly measured from well-resolved scalar separated doublets. This approach is not feasible for the measurement of unresolved proton–proton residual dipolar couplings in partially oriented molecules. Recently, Tjandra *et al.* demonstrated that these proton–proton residual dipolar couplings can be advantageously used for protein NMR structure determination (*8*). Here, we present a novel method to measure such unresolved couplings quantitatively using a coherence transfer scheme that offers an alternative to earlier reports measuring such couplings that may be more difficult to quantitate or are not completely general (*8–12*).

The scheme proposed is shown in Fig. 1. In the following product-operator description, only terms resulting in observable magnetization during the detection period are retained and constant multiplicative factors and relaxation terms are omitted. A three-spin system consisting of an amide proton (H), its directly bound nitrogen (N), and a generic proton (Q) coupled by dipolar (and possibly scalar) coupling to the amide proton will be considered. During the first time period $T$, the chemical shift evolution of Q is obtained in a constant-time fashion. Simultaneously, antiphase proton–proton magnetization, i.e., $2Q_yH_z$ at point $a$ is generated via residual dipolar and scalar coupling between Q and H. After transfer to the amide proton by the second proton 90° pulse ($2Q_zH_y$) the active $^1H$–$^1H$ coupling is refocused during a second period $T$ and simultaneously antiphase coherence $2H_yN_z$ with respect to the directly bound $^{15}N$ nuclei is created ($\tau_1$ is set to $1/4J_{HN}$). Coherence $H_x$ originating on the amide proton H is also frequency labeled during the first constant time period $T$, and acquires antiphase coherence with respect to the directly bound N nucleus in the second period $T$. The two coherences of origins Q and H both follow a path of $^{15}N$ chemical shift evolution during $t_2$ followed by the reverse INEPT to in-phase amide proton magnetization. At the start of the acquisition ($b$ in Fig. 1) the observable components of the density operator are thus given by

$$\sigma(b) = H_y\cos[\Omega_N t_2]*\{\sin^2[\pi\Delta T]\cos[\Omega_Q t_1] + \cos^2[\pi\Delta T]\cos[\Omega_H t_1]\}, \quad [1]$$

where $\Delta$ indicates the residual dipolar coupling between the amide proton H and proton Q. If Q is the intra-residual $^1H^\alpha$ proton, $\Delta$ also contains the three-bond scalar coupling. According to Eq. [1], the ratio of the intensities between the diagonal and the cross-peak yields, neglecting differences in transverse relaxation rates during $t_1$, a good estimation of the residual dipolar coupling $\Delta$ between the involved nuclei. However, because the coupling evolves with the square of the trigonometric functions, the sign of the residual dipolar coupling cannot be retrieved.

Recently, Hansen *et al.* proposed DCOSY (*9*), that uses a TOCSY sequence to observe long range proton–proton correlations via residual dipolar couplings. Although DCOSY can in principle distinguish direct from relay ("spin-diffusion") cross-peaks, it is impossible to deconvolute the simultaneous contribution of these processes to a single peak. This limits the possibility of extracting quantitative information from the DCOSY experiment. More recently, Tian *et al.* (*11*) proposed a CT-COSY experiment that eliminates multiple relay peaks. In this experiment the residual dipolar couplings can, in prin-

[1] Current address: TRIAD Therapeutics, 5820 Nancy Ridge Drive, San Diego, CA 92121.

[2] To whom correspondence should be addressed. E-mail: mpellecchia@triadt.com. E-mail: zuiderwe@umich.edu.



1090-7807/00 $35.00

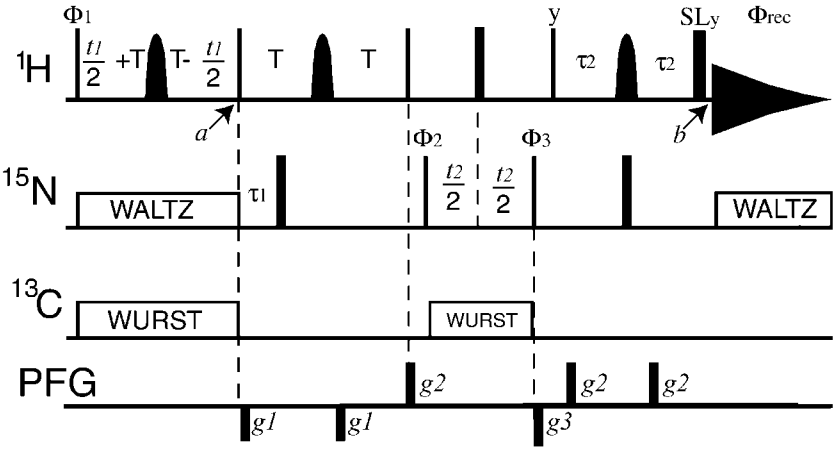


**FIG. 1.** Pulse sequence to measure residual dipolar coupling interactions between protons. Narrow and thin bars represent 90° and 180° rf pulses, respectively. Unless specified otherwise, pulse phases are along the *x*-axis. When working with a perdeuterated protein, or when interested only in $^1H^N$–$^1H^N$ residual dipolar couplings, the $^1H$ carrier position is set to 9.2 ppm throughout the experiment and then shifted to 4.8 ppm prior to acquisition. In this case, the 180° proton pulses in the middle of the INEPT steps are REBURP pulses of 1 ms duration and 6.04 kHz peak amplitude. The pulses are designed to invert the amide proton resonances only and do not perturb the water magnetization that is consequently suppressed by the pulsed field gradients. Also, these selective pulses refocus amide proton to aliphatic proton residual dipolar couplings in protonated proteins. When working with protonated proteins where all proton–proton residual dipolar couplings are of interest, the $^1H$ carrier is set at the water resonance except during the final INEPT transfer, and the 180° proton pulses in the middle of the two time periods-2T are nonselective. The pulsed field gradients are of 1 ms duration and strengths of $g_1 = -30$ G/cm, $g_2 = 38$ G/cm, $g_3 = -38$ G/cm. The delays are $T = 10$ ms for YopH and 5 ms for DnaK, $\tau_1 = \tau_2 = 2.6$ ms. States–TPPI quadrature detection in $t_1$ and $t_2$ was achieved by incrementing $\phi_1$ and $\phi_2$, respectively. $^{15}N$ decoupling during $t_1$ was obtained with a 2.0 kHz WALTZ-16 decoupling sequence. The $^{15}N$ resonances were decoupled from both $^{13}C\alpha$ and $^{13}CO$ by a WURST decoupling sequence (*25*) based on two CAWURST-20 shaped pulses of 10 ms duration covering 4000 Hz bandwidth each, one at the C$\alpha$ frequency and one shifted by 24 000 Hz. WURST adiabatic homonuclear decoupling (*24–26*) was applied during acquisition for the data shown in Fig. 4. A spin lock pulse (10 $\mu$s to 1 ms) prior to data acquisition was employed to improve the solvent suppression. Phase cycle: $\phi_1 = 2(y), 2(-y)$; $\phi_2 = x, -x$; $\phi_3 = 4(x), 4(-x)$ $\Psi_{rec} = x, -x, -x, x, -x, x, x, -x$.

ciple, be obtained from the intensity ratio of the cross-peaks and diagonal. However, as the cross-peaks in their experiment have an anti-phase or phase-shifted character, they are difficult to integrate (*9*). The method reported by Cai *et al.* (*12*) is not completely general as it measures $^1H^N$–$^1H^\alpha$ couplings only. Very recently, Tjandra *et al.* (*8*) report the use of a HNHA experiment for the quantitation of $^1H$–$^1H$ dipolar couplings. The appearance, as well as information content, of their experiment is very similar to our proposed experiment. But, our experiment can be easily adapted for larger molecules by using a TROSY scheme (*13–15*) instead of the HSQC sequence shown. In addition, for perdeuterated protein samples, a $S^3E$-based single-spin-transition selection (*16*) during the $t_1$ period can also be implemented, which will select the narrow components of the $^1H^N$ doublets in that dimension. This method was recently demonstrated by Pervushin *et al.* (*17*).

As an application, we recorded the experiment with a 0.3 mM sample of $^2H/^{15}N/^{13}C$ labeled Yersinia Outer Protein H (YopH, 15 kDa molecular weight) dissolved in an aqueous solution containing 6.0% DMPC/DHPC/CTAB at 3.2:1:0.1 ratio (*18*). With the fully deuterated sample only amide-proton-to-amide-proton correlations are possible. Figure 2 shows examples of some of the observed cross-peaks, between Glu 71 and Asp 72 and between Thr 73 and Ala 74 in Fig. 2A, and the inter-strand $^1H^N$(Ser102)–$^1H^N$(Asp89) connectivities in Fig. 2B. Using the assumption of identical relaxation, the observed dipolar couplings were measured for all cross-peaks of YopH with Eq. [1], and compared with corresponding distances in the three-dimensional structure of YopH (C. Smith and M. A. Saper, personal communication) (Table 1). For YopH, the experiment shows strong cross-peaks only for protons that are separated by not more than 3.0–3.5 Å, with an average residual dipolar coupling of 6.3 Hz. This limited range is perhaps surprising, as it has been claimed that, because of the $r^{-3}$ dependence of the residual dipolar couplings (*1*), proton–proton correlations via residual dipolar couplings may be exploited to cover larger distances than those obtainable via the nuclear Overhauser effect, which is a function of $r^{-6}$. However, residual dipolar couplings affect transverse magnetization only, and the transfer efficiency is severely limited by the $^1H$ transverse relaxation time $T_{2H}$. Even for medium-sized macromolecules, this is much smaller than the longitudinal relaxation time $T_{1H}$ which limits the efficiency of NOE transfer. However, for smaller molecules approaching the extreme narrowing limit, the NOE effect approaches zero, whereas the average $T_{2H}$ values approach $T_{1H}$ and are relatively long. In this situation we can foresee that the magnetization transfer via residual dipolar couplings can indeed provide longer-range information that may not be otherwise accessible.

For our sample conditions, we observe almost exclusively sequential $^1H^N$–$^1H^N$ transfers for residues in helical areas of the protein (Table 1). Moreover, because of the somewhat strin-

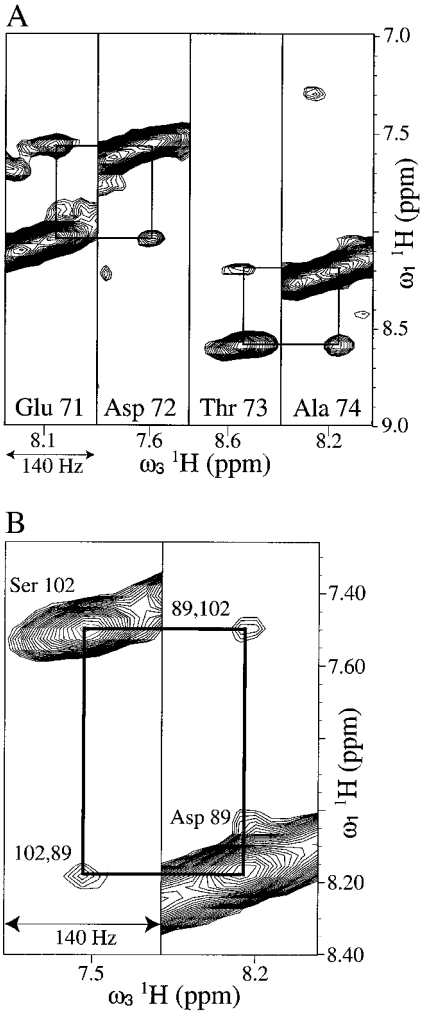


**FIG. 2.** Selected strips taken along $\omega 3$ from a dipolar COSY spectra measured with the scheme of Fig. 1 with a sample of 0.3 mM $^{2}H$, $^{15}N$, $^{13}C$ labeled YopH (15 kDa). The measurements were performed at 305 K with the sample dissolved in an aqueous solution containing 6% DMPC/DHPC/CTAB at 3.2:1:0.1 ratio. The spectra were recorded on a Varian INOVA800 spectrometer operating at 800 MHz $^{1}H$ frequency equipped with a triple resonance probe with a shielded $z$-gradient coil. Forty-two increments were recorded in the first indirect dimension and 25 in the second indirect dimension. The spectra were processed using VNMR and PROSA (*27*) and visualized using XEASY (*28*). (A) Sequential connectivities between residues Glu 71 and Asp 72 and between Thr 73 and Ala 74 typical of the many short-range interactions observed. (B) A cross-strand connectivity in a $\beta$-sheet.

gent angular requirements (*1*), only a subset of these connectivities is observed which correspond to roughly parallel vectors in these helices (Fig. 3). This observation suggests that a mere qualitative assessment of the $^{1}H^{N}$–$^{1}H^{N}$ couplings will be useful for the determination of low-resolution protein folds for fully deuterated proteins as follows. Together with the one-bond $^{1}H$–$^{15}N$ dipolar couplings, which give information about the direction of the helix axis since they report on vectors that are all roughly parallel to that axis, the $^{1}H^{N}$–$^{1}H^{N}$ dipolar couplings yield valuable information on the orientation of the

**TABLE 1**[a]

| $^{1}H^{N}$–$^{1}H^{N}$ connectivities (Res. numbers) | Residual dipolar couplings (Hz) |
|---|---|
| 5–6 (h) | 6.4 ± 0.4 |
| 6–7 (h) | 4.1 ± 0.3 |
| 10–11 (h) | 5.5 ± 0.6 |
| 20–21 (t) | 5.9 ± 0.5 |
| 55–56 (h) | 5.0 ± 0.5 |
| 71–72 (h) | 6.9 ± 0.4 |
| 73–74 (h) | 6.2 ± 0.4 |
| 77–78 (h) | 6.2 ± 0.4 |
| 89–102 (c) | 5.2 ± 0.4 |
| 101–102 (b) | 8.4 ± 0.5 |
| 104–105 (t) | 8.8 ± 0.4 |
| 110–111 (h) | 6.6 ± 0.8 |
| 112–113 (h) | 8.3 ± 0.3 |
| 114–115 (h) | 7.6 ± 0.4 |
| 121–122 (h) | 7.9 ± 0.4 |

[a] The secondary structure of the correlated residues is indicated in the first column with *h* for helix, *t* for turn, *b* for $\beta$-sheet bulge, and *c* for anti-parallel $\beta$-sheet cross-strand, according to a preliminary X-ray structure of YopH.

helical faces, as they constrain vectors that lie at various angles from the axis.

Provided that the molecular alignment tensor is known from residual one-bond $^{1}H$–$^{15}N$ dipolar couplings (*19–22*), the $^{1}H$–$^{1}H$ residual dipolar couplings can be used to restrain the length and the orientation of these vectors for structure refinement. It is important to emphasize that the information derived from the dipolar coupling is free from spin-diffusion therefore representing a valuable complement to NOE-derived distance constraints, especially for intra-residue constraints. A very recent paper by Tjandra *et al.* (*8*) shows that such a structure refinement is indeed possible and useful, even for cases where the signs of the dipolar couplings are unknown.

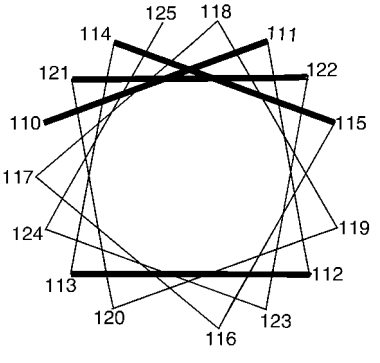


**FIG. 3.** Wheel representation of helix IV (residues 110 to 125) of YopH. The thickness of the lines represent the magnitude of the $^{1}H^{N}$–$^{1}H^{N}$ dipolar couplings observed between the given residues. Thick lines: $\Delta > 4$ Hz (strong sequential connectivities); thin lines $\Delta < 2.5$ Hz (cross-peak not observed). The reported value is the average of the intensity and integral for both strips except when overlapped. The error has been estimated from the noise level of the spectrum.

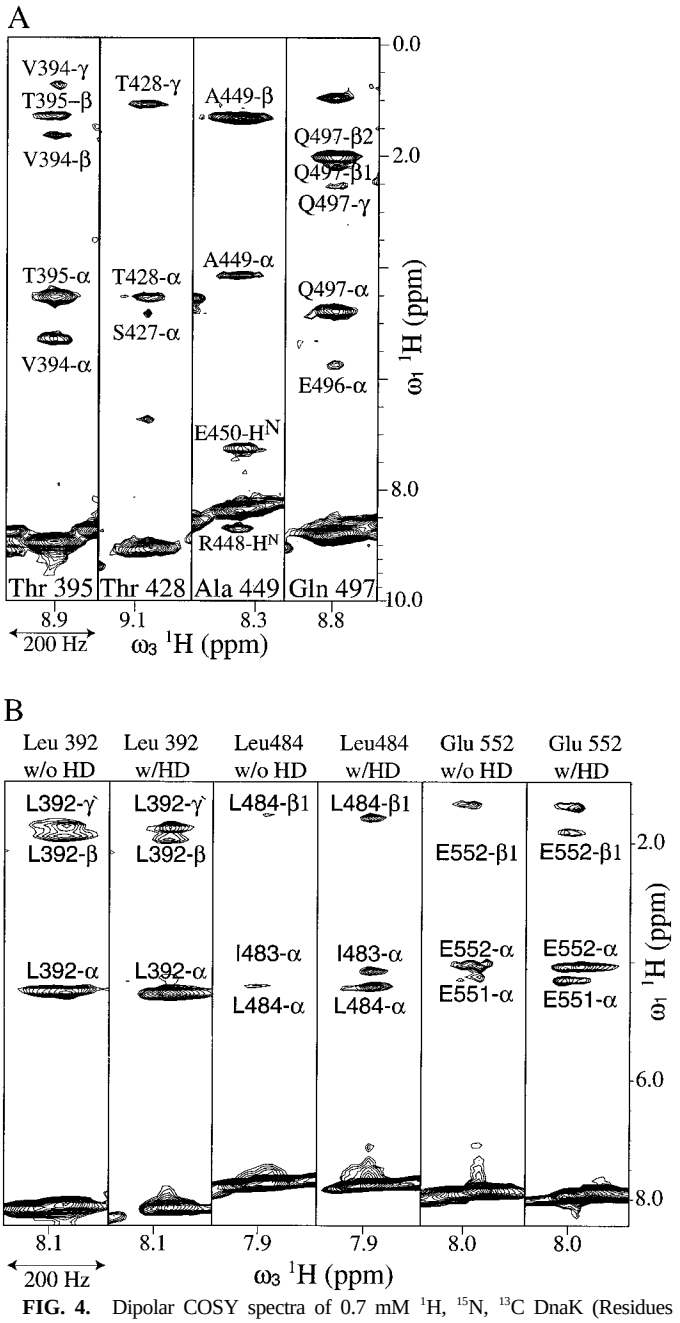


**FIG. 4.** Dipolar COSY spectra of 0.7 mM $^{1}H$, $^{15}N$, $^{13}C$ DnaK (Residues 386–561) recorded with the scheme in Fig. 1. (A) Dipolar COSY spectra of selected amino acids showing amide-side chain and amide-backbone connectivities. The spectrum was recorded using 144 increments in the first indirect dimension and 26 increments in the second indirect dimension. (B) Comparison between dipolar COSY spectra recorded with and without the use of selective homonuclear aliphatic decoupling (*24*–*26*) during acquisition. The nondecoupled spectrum was recorded as described in (A) while the decoupled spectrum was recorded with 128 increments in the first indirect dimension and 25 increments in the second indirect dimension. A 1.6 ms WURST-4 adiabatic decoupling pulse was applied at 2.5 ppm during the $t_3$ evolution which had a bandwidth of 4000 Hz and employed a TPG supercycle used in a four step MLEV-4 cycling (*29*).

In fully protonated proteins many dipolar interactions between amide and aliphatic protons can be observed. This is demonstrated using our new sequence for a $^{15}N/^{13}C$ labeled sample of a 21 kDa domain of the protein chaperone DnaK (*23*). The observed interactions are found to occur almost exclusively between the amide proton and the side-chain protons of the same residue, as well as sequential residues (Fig. 4). Interestingly, one may therefore consider the new experiment as a useful complement to a 3D $^{15}N$-resolved NOESY experiment to aid in spin-system identification and proton side-chain resonance aasignment. In addition, the dipolar interactions contain information about the side-chain conformation. For fully protonated proteins a high degree of alignment also causes significant inhomogeneous broadening of the $^{1}H^{N}$ resonances due to numerous unresolved $^{1}H$–$^{1}H$ residual dipolar couplings. To partially eliminate this problem we have recently demonstrated that amide proton to aliphatic proton residual dipolar couplings are efficiently removed with band-selective homonuclear decoupling during data acquisition (*24*). Figure 4b shows the narrowing effect of such homonuclear decoupling for the current experiment which, in many cases, allows the observation of signals which otherwise did not emerge from the noise.

In conclusion, we present a novel experiment that allows the quantitative measurement of proton–proton residual dipolar couplings in partially aligned proteins. The experiment can be easily combined with TROSY and homonuclear decoupling to study larger proteins at higher degree of alignments and therefore it represents a valid tool for resonance assignment, structure refinement, and determination of low-resolution protein folds.

## ACKNOWLEDGMENTS

The work was supported by NIH Grants GM52421 and GM52406. CWVK is the recipient of a University of Michigan Regents Fellowship. We thank Drs. C. Smith and M. A. Saper for preliminary coordinates of YopH. The W. M. Keck Foundation, NIH, NSF and Parke-Davis/Warner Lambert are gratefully acknowledged for financial support toward the 800 MHz NMR instrument.

## REFERENCES

1. N. Tjandra and A. Bax, Direct measurement of distances and angles in biomolecules by NMR in a dilute liquid crystalline medium, *Science* **278,** 1111–1114 (1997).
2. J. R. Tolman, J. M. Glanagan, M. A. Kennedy, and J. H. Prestegard, Nuclear magnetic dipole interactions in field-oriented proteins: Information for structure determination in solution, *Proc. Natl. Acad. Sci. USA* **92,** 9279–9283 (1995).
3. N. Tjandra, S. Grzesiek, and A. Bax, Magnetic field dependence of nitrogen-proton J splittings in N-15-enriched human ubiquitin resulting from relaxation interference and residual dipolar coupling, *J. Am. Chem. Soc.* **118,** 6264–6272 (1996).
4. C. A. Bewley, K. R. Gustafson, M. R. Boyd, D. G. Covell, A. Bax, G. M. Clore, and A. M. Gronenborn, Solution structure of cyanovirin-N, a potent HIV-inactivating protein, *Nature Struct. Biol.* **5,** 571–578 (1998).
5. A. C. Drohat, N. Tjandra, D. M. Baldisseri, and D. J. Weber, The use

of dipolar couplings for determining the solution structure of rat apo-S100B (beta beta), *Protein Sci.* **8,** 800–809 (1999).

6. M. R. Hansen, L. Mueller, and A. Pardi, Tunable alignment of macromolecules by filamentous phage yields dipolar coupling interactions, *Nature Struct. Biol.* **5,** 1065–1074 (1998).
7. N. Tjandra, J. G. Omichinski, A. M. Gronenborn, G. M. Clore, and A. Bax. Use of dipolar $^{1}H$-$^{15}N$ and $^{1}H$-$^{13}C$ couplings in the structure determination of magnetically oriented macromolecules in solution, *Nature Struct. Biol.* **4,** 732–738 (1997).
8. N. Tjandra, J. Marquardt, and G. M. Clore, Direct Refinement against Proton–Proton Dipolar Couplings in NMR Structure Determination of Macromolecules, *J. Magn. Reson.* **142,** 393–396 (2000).
9. M. R. Hansen, M. Rance, and A. Pardi, Observation of long-range H-1-H-1 distances in solution by dipolar coupling interactions, *J. Am. Chem. Soc.* **120,** 11210–11211 (1998).
10. P. J. Bolon and J. H. Prestegard, COSY cross-peaks from H-1-H-1 dipolar couplings in NMR spectra of field oriented oligosaccharides, *J. Am. Chem. Soc.* **120,** 9306–9307 (1998).
11. F. Tian, P. J. Bolon, and J. H. Prestegard, Intensity-Based Measurement of Homonuclear Residual Dipolar Couplings from CT-COSY, *J. Am. Chem. Soc.* **121,** 7712–7713 (1999).
12. M. Cai, J. Wang, E. T. Olejniczak, R. P. Meadows, A. H. Gunasekera, N. Xu, and S. W. Fesik, Accurate measurements of $H^{N}$–$H^{\alpha}$ residual dipolar couplings in proteins, *J. Magn. Reson.* **139,** 451–453 (1999).
13. K. Pervushin, R. Riek, G. Wider, and K. Wüthrich, Attenuated T-2 relaxation by mutual cancellation of dipole-dipole coupling and chemical shift anisotropy indicates an avenue to NMR structures of very large biological macromolecules in solution, *Proc. Natl. Acad. Sci. USA* **94,** 12366–12371 (1997).
14. M. Czich and R. Boelens, Sensitivity enhancement in the TROSY experiment, *J. Magn. Reson.* **134,** 158–160 (1998).
15. M. Rance, J. P. Loria, and A. G. III Palmer, Sensitivity improvement of transverse relaxation optimized spectroscopy, *J. Magn. Reson.* **136,** 92–101 (1999).
16. A. Meissner, J. O. Duus, and O. W. Sorensen, Spin-State-Selective Excitation. Application for E.COSY-type measurement of $J_{HH}$ coupling constants, *J. Magn. Reson.* **128,** 92–97 (1997).
17. K. V. Pervushin, G. Wider, R. Riek, and K. Wüthrich, The 3D NOESY-[H-1,N-15,H-1]-ZQ-TROSY NMR experiment with diagonal peak suppression, *Proc. Natl. Acad. Sci. USA* **96,** 9607–9612 (1999).
18. J. A. Losonczi and J. H. Prestegard, Improved dilute bicelle solutions for high-resolution NMR of biological macromolecules, *J. Biomol. NMR* **12,** 447–451 (1998).
19. G. M. Clore, A. M. Gronenborn, and N. Tjandra, Direct structure refinement against residual dipolar couplings in the presence of rhombicity of unknown magnitude, *J. Magn. Reson.* **131,** 159–162 (1998).
20. G. M. Clore, A. M. Gronenborn, and A. Bax, A robust method for determining the magnitude of the fully asymmetric alignment tensor of oriented macromolecules in the absence of structural information, *J. Magn. Reson.* **133,** 216–221 (1998).
21. Y. X. Wang, J. L. Marquardt, P. Wingfield, S. J. Stahl, S. Lee-Huang, D. Torchia, and A. Bax, Simultaneous measurement of $^{1}H$-$^{15}N$, $^{1}H$-$^{13}C$, and $^{15}N$-$^{13}C$ dipolar couplings in a perdeuterated 30 kDa protein dissolved in a dilute liquid crystalline phase, *J. Am. Chem. Soc.* **120,** 7385–7386 (1998).
22. J. A. Losonczi, M. Andrec, M. W. F. Fischer, and J. H. Prestegard, Order matrix analysis of residual dipolar couplings using singular value decomposition, *J. Magn. Reson.* **138,** 334–342 (1999).
23. H. Wang, A. V. Kurochkin, Y. Pang, W. D. Hu, G. C. Flynn, and E. R. P. Zuiderweg, NMR solution structure of the 21 kDa chaperone protein DnaK substrate binding domain: A preview of chaperone-protein interaction, *Biochemistry* **37,** 7929–7940 (1998).
24. C. W. Vander Kooi, E. Kupce, E. R. P. Zuiderweg, and M. Pellecchia, Line narrowing in spectra of proteins dissolved in a dilute liquid crystalline phase by band-selectrive adiabatic decoupling: Application to $^{1}H^{N}$-$^{15}N$ residual dipolar coupling measurements, *J. Biomol. NMR* **15,** 335–338 (1999).
25. E. Kupce and R. Freeman, Adiabatic pulses for wide-band inversion and broad-band decoupling, *J. Magn. Reson. A* **115,** 273–276 (1995).
26. E. Kupce and G. Wagner, Wideband homonuclear decoupling in protein spectra, *J. Magn. Reson. B* **109,** 329–333 (1995).
27. P. Güntert, V. Dötsch, G. Wider, and K. Wüthrich, Processing of multidimensional NMR data with the new software PROSA, *J. Biomol. NMR* **2,** 619–629 (1992).
28. C. Bartels, T. Xia, M. Billeter, P. Güntert, and K. Wüthrich, The program XEASY for computer-supported NMR spectral-analysis of biological macromolecules, *J. Biomol. NMR* **6,** 1–10 (1995).
29. M. H. Levitt and R. Freeman, Composite pulse decoupling, *J. Magn. Reson.* **43,** 502–507 (1981).